



## Letter

## Organic light-emitting diodes based on an ambipolar single crystal

Xianjie Li, Yuanxiang Xu, Feng Li\*, Yuguang Ma\*

State Key Lab of Supramolecular Structure and Materials, Jilin University, 2699 Qianjin Avenue, Changchun 130012, People's Republic of China

## ARTICLE INFO

## Article history:

Received 18 October 2011

Received in revised form 20 December 2011

Accepted 29 January 2012

Available online 10 February 2012

## Keywords:

Slice-like organic single crystal

Charge transport

Time of flight technique

Organic light-emitting diode

## ABSTRACT

Slice-like organic single crystals of 1,4-bis(2-cyano-2-phenylethenyl)benzene (BCPEB) are grown by the physical vapor transport (PVT) method, and exhibit a very high photoluminescence quantum efficiency ( $\Phi_{\text{PL}}$ ) of 75%. The ambipolar behavior of BCPEB single crystals are confirmed using the time of flight technique. The high efficiency and balanced ( $\mu_{\text{h}} = 0.059 \text{ cm}^2/\text{Vs}$  and  $\mu_{\text{e}} = 0.070 \text{ cm}^2/\text{Vs}$ ) carriers' mobility imply that the BCPEB single crystal is a promising light-emitting layer in the diodes structure. Intense green electroluminescence (EL) from a diode has been successfully demonstrated at an applied electric field of  $2 \times 10^5 \text{ V/cm}$ .

© 2012 Elsevier B.V. All rights reserved.

## 1. Introduction

Organic single crystals have attracted much attention as organic optoelectronic materials since 1960s [1–2]. Light-emitting diodes (LEDs) based on anthracene single crystals were successfully fabricated during that time. However, the diodes showed very high driving voltage beyond 100 V to get the electroluminescence (EL), due to the low photoluminescence quantum efficiency ( $\Phi_{\text{PL}}$ ) and large thickness (approximately 1 mm) of anthracene single crystals [2]. Recently, slice-like organic single-crystals (usually 0.5–10  $\mu\text{m}$ ), such as oligo (p-phenylenevinylene) (OPV) [3–8] and thiophene/phenylene co-oligomers (TPCOs) [9–13] combining both high carriers' mobility and high  $\Phi_{\text{PL}}$  has been developed and grown by the physical vapor transport (PVT) method [14]. In particular, light-emitting field-effect transistors (FETs) [5,6,10,11,13] based on these single crystals have been made great progress, while LEDs based on them are still scarce [7,9,15].

In this letter, slice-like OPV single crystals of 1,4-bis(2-cyano-2-phenylethenyl)benzene (BCPEB) are grown by the PVT method. They have high  $\Phi_{\text{PL}}$  (up to 75%) as well

as high carriers' mobility (over  $0.01 \text{ cm}^2/\text{Vs}$  for both electrons and holes). Meanwhile, they have large sizes, regular shape, and flat surfaces. In addition, they are flexible and bendable, thus can easily adhere to the substrate/electrode to provide high-quality electronic contacts. All these properties indicate that they are the promising candidate as the light-emitting layer of LEDs. Then the LEDs based on them are fabricated. The device structure is Au/BCPEB crystal/cathode (Al, LiF/Al). We find that the cathode strongly affect the I–V characteristics. Intense EL is observed at an electric field of above  $2 \times 10^5 \text{ V/cm}$  (correspond to 14 V) with the cathode of LiF/Al at room temperature under ambient condition. As well known, organic single crystals combining high carrier mobility and high  $\Phi_{\text{PL}}$  are promising materials for organic laser diodes (LDs) [5–13], and our results pave a way toward the organic LDs.

## 2. Experimental

BCPEB was synthesized according to the procedure shown in the insert of Fig. 1. All chemicals were purchased commercially, and used without further purification. The mixture of Benzylcyanide (201 mg, 1.5 mmol) and Terephthalaldehyde (0.345 mL, 3 mmol) in tert-butyl alcohol (10 mL) was stirred at 46 °C for 30 min. Then, potassium tert-butoxide (1 M solution in tetrahydrofuran, 0.25 mL)

\* Corresponding authors. Tel.: +86 4315168492; fax: +86 43185193 421.

E-mail addresses: [lifeng01@jlu.edu.cn](mailto:lifeng01@jlu.edu.cn) (F. Li), [ygma@jlu.edu.cn](mailto:ygma@jlu.edu.cn) (Y. Ma).

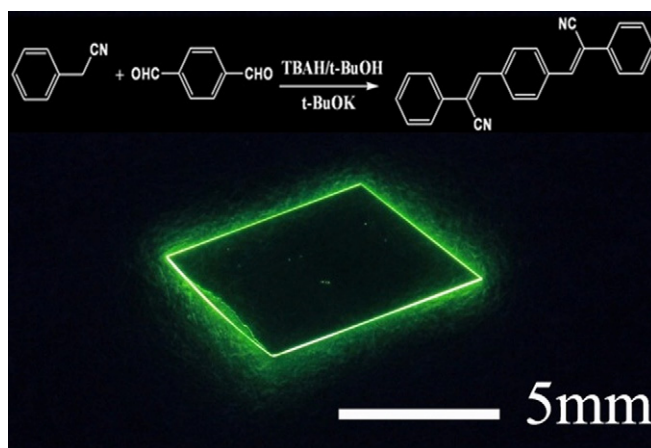


Fig. 1. Fluorescence photograph of a large size ( $5 \times 8$  mm) slice-like BCPEB single crystal. Insert: The BCPEB molecule synthetic scheme.

and tetrabutylammonium hydroxide (TBAH, 1 M solution in methanol, 0.25 mL) were added, and stirred for 20 min. The resulting precipitate was filtered and purified by column chromatography using dichloromethane. BCPEB powder (348 mg) was obtained in yield of 70% by evaporated the solvent.  $^1\text{H NMR}$  ( $\text{CDCl}_3$ )  $\delta$  [ppm]: 8.01 (s, 4H, Ar-H), 7.72–7.71 (d, 4H, Ar-H), 7.56 (s, 2H, Vinyl-H), 7.49–7.46 (t, 4H, Ar-H), 7.44–7.43 (t, 2H, Ar-H). NMR spectra were recorded on Bruker AVANCE 500 MHz spectrometer with chloroform-d as solvent and tetramethylsilane (TMS) as internal standard. Absorption and photoluminescence (PL) spectra were measured using UV-3100 and RF-5301 PC spectrophotometers, respectively. The  $\Phi_{\text{PL}}$  was obtained in an integrating sphere [16]. The X-ray diffraction experiment was performed on a Bruker D8 with GADDS X-ray diffractometer with Cu-K $\alpha$  radiation ( $\lambda = 1.5418 \text{ \AA}$ ) at 40 kV and 20 mA. Atomic force microscopy (AFM) images were taken by tapping mode using a Nanoscope III, Digital Instrument system equipped with a  $5 \times 5 \mu\text{m}$  scanner and a silicon nitride tip. All measurements were carried out at room temperature under ambient conditions.

Slice-like crystals of BCPEB were prepared by the PVT method. During the process of the single-crystal growth, the source zone temperature, grown zone temperature, and gas flow rate were 248 °C, 160 °C, and 30 mL/min, respectively. After several hours of stable growth, the slice-like crystals were found hang inside the growth tubes. The typical thickness of the slice-like crystals was around 0.5–10  $\mu\text{m}$ , as characterized by a Dektak profilometer.

To explore the charge-transporting properties of BCPEB single crystals, we used the TOF technology to measure the carriers' mobility [17]. Samples for TOF measurement had a structure of ITO/PEDOT: PSS (40 nm)/BCPEB ( $d$ )/Al (100 nm), where  $d$  was the thickness of the single crystals. A 40-nm-thick PEDOT: PSS layer was spin-coated on the cleaned indium tin oxide (ITO) coated glass substrate. The selected single crystals with a thickness of several microns were electrostatically laminated on the substrate. Finally, a 100-nm-thick of aluminum layer was deposited through a shadow mask to make an active area of  $1 \text{ mm}^2$ . A Nd:YAG laser ( $\lambda = 355 \text{ nm}$ , pulse width: 10 ns) was used

as the light source for the photo-generating charge carriers. For the holes TOF measurement, the charge carriers were generated near the ITO contact when a positive voltage was applied. Then the holes moved toward the Al contact, and the corresponding displacement current was measured across the load resistor using a digital storage oscilloscope (DPO7104; bandwidth: 1 GHz). In contrast, the electron mobility could be obtained by negatively biasing to the ITO contact. The carriers' mobility was deduced from the transit time  $\tau_{\text{tr}}$  via the equation  $\mu = d^2/V\tau_{\text{tr}}$ , where  $d$  was the thickness of the single crystal, and  $V$  was the applied voltage.

The slice-like crystals with a thickness of several microns were selected for the LEDs fabrication. A 10-nm-thick gold anode was thermally deposited through a shadow mask on a cleaned glass substrate. The crystal was then electrostatically bonded onto the anode. Finally, various cathodes of Al, LiF/Al were thermally deposited on the fixed crystal. The light-emitting area of the devices was  $0.15 \times 1 \text{ mm}^2$ , as defined by a shadow mask. Current density ( $J$ )–electric field ( $E$ )–luminance ( $L$ ) characteristics were measured by using a dual-channel source meter (Keithly 2612). EL spectra were recorded with a fiber spectrometer (Ocean Optics). All the measurements were carried out at room temperature under ambient conditions.

### 3. Results and discussion

Fig. 1 shows the fluorescence photograph of a large size ( $5 \times 8$  mm) slice-like crystal. The crystal shows strong edge emission in the green spectral region with a high  $\Phi_{\text{PL}}$  up to 75%. The absorption spectra of the BCPEB vacuum-deposited film and the PL spectra of the crystal are shown in the upper left insert of Fig. 2. BCPEB displays absorption peak at 309 nm as film and PL peak at 531 nm in the crystal, respectively. The AFM measurement (Fig. 2) shows that the surface of the slice-like crystal is very smooth except the layer-by-layer steps near the crystal edges. From the cross section analysis, the vertical height of one step is 1.92 nm. Wide-angle X-ray diffraction

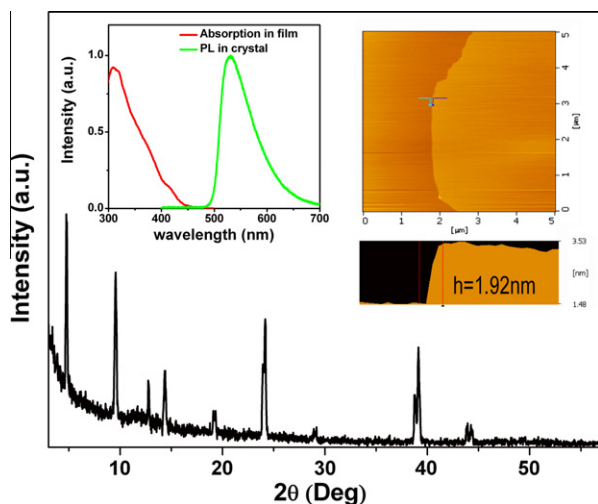
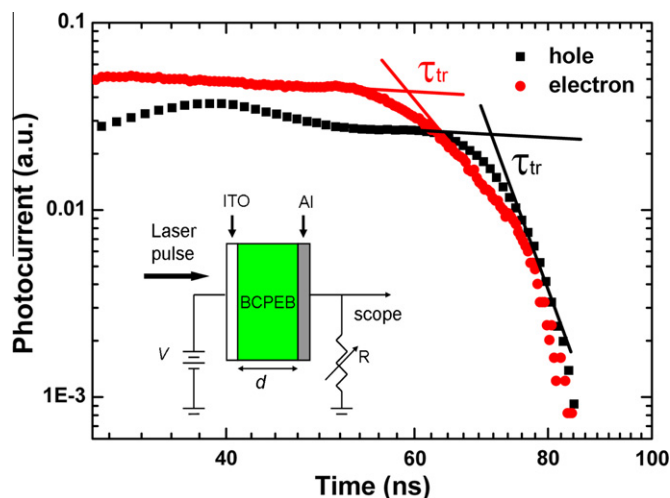


**Fig. 2.** XRD pattern of the BCPEB single crystal. Insert (upper left): Absorption spectra of BCPEB vacuum-deposited film and photoluminescence spectra of BCPEB single crystal. Insert (upper right): The BCPEB slice-like crystal surface AFM height images.

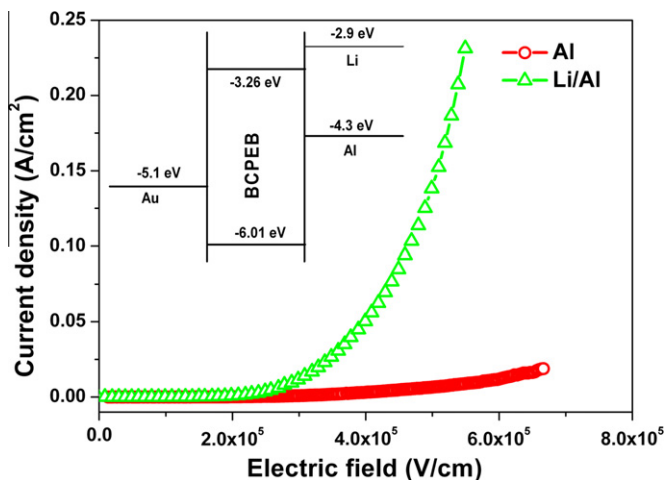
(XRD) is a powerful technique to determine the molecular layer-by-layer structure. Fig. 2 shows the diffraction patterns of XRD on the slice-like crystals. As can be seen, the diffraction peaks occur equidistantly with varying angle degree and the diffraction peaks are very sharp, so these slice-like crystals should have good ordered layer structures. According to the Bragg equation, the thickness of a layer is calculated to be 1.88 nm which is consistent well with the step height in the AFM image. Moreover, the value of 1.88 nm approximates to the length of the long-axis of the BCPEB molecule (1.79 nm), indicating that the long-axis of the molecule is perpendicular to the surface of the slice-like crystal.

Fig. 3 shows the TOF transient photocurrent of the holes (black squares) and electrons (red circles) in the single crystal with a thickness of 4 μm. A schematic diagram of the TOF measurement was also shown (Fig. 3). The transit time of the holes and electrons are 68 ns and 57 ns with an applied voltage of 40 V, respectively. The obtained hole and electron mobilities are 0.059 cm<sup>2</sup>/Vs and 0.070 cm<sup>2</sup>/Vs, which are comparable to the previously reported values of OPV single crystals [7,8]. The balanced hole and electron mobility indicate that the BCPEB single crystal possessed the ambipolar property which benefits the dual charge transport and recombination in the diode structure.

Fig. 4 shows the *J*-*E* characteristics of the slice-like crystal LEDs with the structure of Au/BCPEB crystal/cathode (Al, LiF/Al). The Au electrode was chosen as an anode for two reasons. First, as shown in the energy level diagram (Fig. 4), the work function of Au is -5.1 eV which is much lower than other metals (Ag, Al), thus the injection barrier for hole carriers is the lowest; second, we found that the slice-like crystal can spontaneously and tightly adhere to the Au anode. As can be seen from Fig. 4, the device with the LiF/Al cathode performs better. Its current density at the electric field of 5 × 10<sup>5</sup> V/cm is one order of magnitude higher than that of the device with a pure Al cathode. Both the devices with the two different cathodes show EL at the electric field of above 10<sup>5</sup> V/cm. The LiF/Al electrodes have been widely used in OLEDs [18,19], the underlying mechanisms are still under investigation. One possible explanation is that LiF is dissociated during thermal deposition in the presence of water molecules, and forms Li-Al alloys at the interface between LiF/Al and BCPEB single crystal. As shown in the insert of Fig. 4, there is no electron injection barrier at the interface between Li and BCPEB single crystal, while the electron injection barrier at the interface between Al and BCPEB single crystal is 1.04 eV. Consequently, the devices with LiF/Al cathode exhibit much better *J*-*E* characteristics.



**Fig. 3.** Time-of-flight transient photocurrent of the holes (black squares) and electrons (red circles) in the BCPEB single crystal with a thickness of 4 μm. Insert: A schematic diagram of the time-of-flight measurement. (For interpretation of the references to colour in this figure legend, the reader is referred to the web version of this article.)



**Fig. 4.** Current density ( $J$ )–electric field ( $E$ ) characteristics of the BCPEB single-crystal OLEDs with the structure of Au/BCPEB crystal/cathode (Al, LiF/Al). Inset: Energy level diagram of the single-crystal based OLEDs.

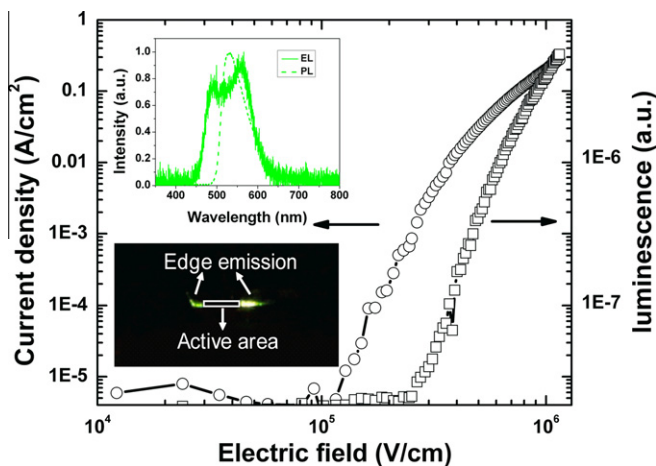


**Fig. 5.** Current density ( $J$ )–electric field ( $E$ )–luminescence ( $L$ ) characteristics of the BCPEB single-crystal OLEDs with the structure of Au/BCPEB crystal ( $0.7 \mu\text{m}$ )/LiF/Al. Inset (lower left): photograph of the EL edge emission. Inset (upper left): EL spectrum of BCPEB single-crystal and the PL spectrum of BCPEB single-crystal as reference.

Fig. 5 shows the  $J$ – $E$ – $L$  characteristics of the slice-like crystal LEDs with the structure of Au/BCPEB crystal ( $0.7 \mu\text{m}$ )/LiF/Al. We can see that the carriers start to inject and transport at an electric field of  $1 \times 10^5 \text{ V/cm}$ , which is comparable to the conventional amorphous thin-film OLEDs. Light emission was observed at an electric field around  $2 \times 10^5 \text{ V/cm}$  (correspond to 14 V). The maximum current density is limited to only  $0.3 \text{ A/cm}^2$  due to the breakdown of the devices or the cathode detached from the crystal. The photograph of the EL emission is shown in the lower left insert of Fig. 5. Although the top emission was blocked by the thick LiF/Al layer, intense green EL was still observed from the edge of the diode. In addition, the EL spectrum of the edge emission is shown in the upper left insert of Fig. 5. The shape of the EL spectrum has a little

difference from the PL spectrum, which may be caused by the light propagation in the waveguide structure.

#### 4. Conclusion

Slice-like single crystals of BCPEB with high  $\Phi_{\text{PL}}$  are grown by PVT method. The slice-like crystals are flexible and bendable, and thus easily adhere to the substrate/electrode to create better interfacial contacts in the fabrication of the diode. The mobility deduced from the time-of-flight (TOF) measurements for holes and electrons are high and balanced, which are essential to achieving high EL efficiency of LEDs. Finally, we have successfully demonstrated the slice-like crystal based LED by using LiF/Al cathode and

observed the intense green EL from the edge of the device. The results indicate that the slice-like crystals are promising candidate to make organic single-crystal based LEDs.

### Acknowledgment

We are grateful for financial support from the National Science Foundation of China (Grant numbers 50733002, 60878013, 20921003).

### References

- [1] M. Pope, H.P. Kallmann, P. Magnante, *J. Chem. Phys.* 38 (1963) 2042.
- [2] W. Helfrich, W.G. Schneider, *Phys. Rev. Lett.* 14 (1965) 229.
- [3] Z.Q. Xie, B. Yang, F. Li, G. Cheng, L.L. Liu, G.D. Yang, H. Xu, L. Ye, M. Hanif, S.Y. Liu, D.G. Ma, Y.G. Ma, *J. Am. Chem. Soc.* 127 (2005) 14152.
- [4] W.J. Xie, Y.P. Li, F. Li, F.Z. Shen, Y.G. Ma, *Appl. Phys. Lett.* 90 (2007) 141110.
- [5] H. Nakanotani, R. Kabe, M. Yahiro, T. Takenobu, Y. Iwasa, C. Adachi, *Appl. Phys. Exp.* 1 (2008) 091801.
- [6] H. Nakanotani, M. Saito, H. Nakamura, C. Adachi, *Appl. Phys. Lett.* 95 (2009) 103307.
- [7] H. Nakanotani, C. Adachi, *Appl. Phys. Lett.* 96 (2010) 053301.
- [8] H. Wang, F. Li, I. Ravia, B.R. Gao, Y.P. Li, V. Medvedev, H.B. Sun, N. Tessler, Y.G. Ma, *Adv. Funct. Mater.* 21 (2011) 3770.
- [9] M. Ichikawa, K. Nakamura, M. Inoue, H. Mishima, T. Haritani, R. Hibino, T. Koyama, Y. Taniguchi, *Appl. Phys. Lett.* 87 (2005) 221113.
- [10] T. Takenobu, S.Z. Bisri, T. Takahashi, M. Yahiro, C. Adachi, Y. Iwasa, *Phys. Rev. Lett.* 100 (2008) 066601.
- [11] S.Z. Bisri, T. Takenobu, Y. Yomogida, H. Shimotani, T. Yamao, S. Hotta, Y. Iwasa, *Adv. Funct. Mater.* 19 (2009) 1.
- [12] S. Hotta, T. Yamao, *J. Mater. Chem.* 21 (2011) 1295.
- [13] Y. Yomogida, T. Takenobu, H. Shimotani, K. Sawabe, S.Z. Bisri, T. Yamao, S. Hotta, Y. Iwasa, *Appl. Phys. Lett.* 97 (2010) 173301.
- [14] Z.Q. Xie, Y.T. Wang, Y.G. Ma, J.C. Shen, *Synth. Met.* 137 (2003) 983.
- [15] K.W. Yee, M. Yokoyama, M. Hiramoto, *Appl. Phys. Lett.* 88 (2006) 083511.
- [16] Y. Kawamura, H. Sasabe, C. Adachi, *J. Appl. Phys.* 43 (2004) 2.
- [17] R.G. Kepler, *Phys. Rev.* 119 (1960) 1226.
- [18] L.S. Hung, C.H. Chen, *Mater. Sci. Eng. R.* 39 (2002) 143.
- [19] X.Y. Deng, S.W. Tong, L.S. Hung, Y.Q. Mo, Y. Cao, *Appl. Phys. Lett.* 82 (2003) 3104.